9.3 A680 μw Burst-Chirp UWB Radar Transceiver for Vital Signs and Occupancy Sensing up to 15m Distance

Liu, Yao-Hong; Sheelavant, Sunil; Mercuri, Marco; Mateman, Paul; Dijkhuis, Johan; Zomagboguelou, Wilfried; Breeschoten, Arjan; Traferro, Stefano; Babaie, Masoud; More Authors

DOI
10.1109/ISSCC.2019.8662536

Publication date
2019

Document Version
Final published version

Published in
2019 IEEE International Solid-State Circuits Conference, ISSCC 2019

9.3 A 680μW Burst-Chirp UWB Radar Transceiver for Vital Signs and Occupancy Sensing up to 15m Distance

Yao-Hong Liu[1], Sunil Sheelavant[1,2], Marco Mercuri[1], Paul Mateman[1], Johan Dijkhuis[1], Wilfried Zomagboguelou[1,3], Arjan Breeschoten[1], Stefano Traferro[1], Yan Zhan[1], Tom Torf[4], Christian Bachmann[1], Pieter Harpe[3], Masoud Babaie[2]

[1]imec - Netherlands, Eindhoven, The Netherlands
[2]Delft University of Technology, Delft, The Netherlands
[3]TU Eindhoven, Eindhoven, The Netherlands
[4]imec, Leuven, Belgium

For remote vital signs and occupancy detection in many smart home/building applications, radar sensors are a preferred option over cameras, due to privacy preservation and robustness to ambient light conditions. These radars not only need to provide precise range and vital signs information over meters distance, but also preferably can operate on a battery up to a few months or even years, for cost and practical reasons (like smoke detectors). State-of-the-art remote vital-sign sensors typically use an impulse-radio UWB (IR-UWB) radar [1,2] because it provides a range resolution <20cm. However, their power consumption is typically in the order of 100's of mW, preventing long-term maintenance-free battery-powered operations. Although mains power can be used to supply such radars, this is not always available, depending on the location and the building type, and the installation cost (e.g., power routing) is significantly higher than for battery-powered ones. In this work, a burst-chirp radar with an energy-efficient chirp generation is proposed, leading to a record-low power consumption of 680μW.

The radar frequency is chosen to be 7GHz UWB for the following reasons: availability of sufficient BW to reach a fine range resolution, possibility of low-power circuit implementation, and lower path loss compared to mm-wave bands. However, UWB has very tough peak (0dBm/50MHz), average (-41dBm/MHz), and sideband (<-70dBm/MHz) power spectral density (PSD) regulations, and the BW is much narrower in certain regions (e.g., 6 to 8.5GHz in Europe). Hence, it is challenging for the IR-UWB radars to fulfill the sidelobe PSD without compromising detection distance [1,2]. Moreover, the power consumption of IR-UWB transceivers does not reduce with the duty cycling. E.g., the IR-UWB RX needs to be continuously active for >66ns to receive a 2ns impulse reflected from a 10m distance (33× longer than the signal duty-cycle). Frequency-modulated continuous-wave (FMCW) radars [3][4] have low sideband emission (<-30dB), but the continuous operation of FMCW radars can easily violate the UWB average PSD requirement compared to IR-UWB radars with a similar detection distance. In this work, an FMCW radar is heavily duty-cycled to a short burst to meet UWB regulations. However, such burst operation also poses several design challenges in FMCW radars: fast chirp generation, frequency pulling, and settling overhead mitigation.

The maximum unambiguous velocity of the targets determines the required pulse repetition interval (PRI) in FMCW radars. A PRI of 1.3ms is chosen here to capture any fast movement of an indoor subject (e.g., sudden falling) with a Doppler velocity up to 7m/s. With 0dBm PA output power, a duty cycling factor should be less than 3% to meet the UWB average PSD restriction, thus resulting in a 40μs chirp time. All the radar circuits are disabled outside the burst-chirp period (Fig. 9.3.1), which significantly reduces the average power consumption by ~33×, whereas the chirp speed should also be increased by the same ratio. Although the 2-point modulation PLL presented in [5] can provide a chirp slope up to 940MHz/29μs, long settling time and high power consumption of the fractional-N PLL significantly increase the energy overhead in a heavy duty-cycling system. A fast chirp generation based on an open-loop DCO is employed in this work, since a precise center frequency is not required and PLLs typically do not rule the fast chirp behavior in a short burst. As shown in Fig. 9.3.1, the DCO is first locked to an initial frequency f0 within 5μs by an FLL consuming 500μW. Then the loop is opened, and the DCO frequency starts to chirp to the targeted final frequency f1. The digital PA (DPA) is only enabled during DCO chirping (Fig. 9.3.1). If the DPA is enabled while the DCO is not chirping, even a 100ns duration would introduce a spur in the spectrum and violate the regulations. On the other hand, if the DPA is activated/deactivated while the DCO is chirping, the frequency pulling would introduce a large chirp frequency error. To alleviate the frequency pulling while avoiding spurs, the DPA is digitally ramped up/down at the start/end of each chirp, and the timing of this procedure is precisely controlled by a finite-state-machine (FSM) with a 20ns time resolution.

Figure 9.3.2 shows the proposed LC-DCO with an embedded Domino chirp generation sampled at 50MHz. The DCO consists of a 9b binary FLL bank and a 9b unary chirp bank. The chirp bank has a digitally-controlled capacitor array with 32 columns and 16 rows, and each unit has a 0.5fF capacitance. If each unit is controlled separately, there will be up to 512 digital controls routing inside the DCO, which would significantly increase parasitics. This will diminish not only the chirp speed, but also the DCO start-up margin. In this work, the dynamic-latch-based shift register is tightly integrated with a unit capacitor, so the entire DCO becomes very compact. To minimize clock activity and also supply droop, only one row at a time has an active clock while the other rows remain static. The chirp slope can reach maximum 700MHz/10μs. During the burst, the FLL, DCO and chirp generation consume only 3mW DC power.

To meet the targeted displacement accuracy for heartbeat detection at several meters, an RMS frequency error must be <2MHz. However, the chirp non-linearity due to the nature of $\sqrt{LC}$ (Fig. 9.3.3) can introduce a frequency error of more than 10MHz. Such non-linearity is predictable, since the FLL precisely defines the initial C0, and the inductance L is fairly constant over PVT. A simple digital predistortion (DPD) technique could have been applied, but the capacitor units in Domino chirp generation are not individually accessible. As conceptually illustrated in Fig. 9.3.3 (with exaggeration), a time-domain DPD (T-DPD) is proposed to correct the curvature of the chirp by modulating the number of the clock periods T_{CLK} in each frequency step k. This number is calculated by a 3rd-order polynomial, which is implemented in the digital domain with simple hardware to approximate the inverse of the square-root relation. The polynomial's coefficients are only adapted for each wafer (i.e., one-time calibration) to overcome the process variation of the unit capacitors (ΔC). The linearized results are insensitive to supply and temperature variations, thanks to the metal-finger capacitors.

An HPF in the RX is typically required in FMCW radars to suppress the TX-RX leakage, but its slow settling significantly increases energy consumption overhead in burst operation. Thanks to the fast chirp slope of 700MHz/40μs, an HPF corner as high as 200kHz can be selected, resulting in a quick settling within 5μs. Unlike the ADCs in many direct-sampling IR-UWB RXs that typically sample at 10s of GHz, and consume 10s of mW [1], the presented radar RX uses a 9b SAR-ADC sampled at 12.5MHz consuming only 30μW.

The chip was fabricated in 40nm CMOS, and the die micrograph is shown in Fig. 9.3.7. Thanks to a digital-intensive implementation, the transceiver occupies a core area of only 0.48mm^2. The TX output spectrum, the time-domain waveform of the TX burst, and its corresponding frequency demodulation are shown in Fig. 9.3.4. When PRI is selected to be 1.3ms, the 0dBm TX has average and sideband PSDs of -45dBm/MHz and -85dBc/MHz, respectively, which are well below the UWB indoor regulations internationally. As shown in Fig. 9.3.5, the chirp non-linearity is dramatically reduced when T-DPD is applied, and the results are fairly consistent against supply and temperature variations. The measured RMS error among 5 different dies in the same wafer is 0.3 to 0.5MHz. The measured RX P_{1dB} and noise figure are -35dBm and 12.5dB, respectively. Figure 9.3.5 also shows the RX output de-chirping FFT with rectangular windowing. A 3m cable delay and a 50dB attenuator are connected in between TX output and RX input. The measured sidelobe is lower than -12.8dB after applying T-DPD, where the ideal level is -13.5dB [4]. The presented radar together with off-the-shelf antennas (each 16cm^2 size, 3-to-6dB gain) can detect human respiration and heartbeat up to 15meter and 5meter distances, respectively. The peak power consumption is broken down in Fig. 9.3.5. Even lower average power consumption can be achieved with longer PRI for slow-moving scenarios. Figure 9.3.6 summarizes the performance and compares with state-of-the-art IR-UWB and FMCW radars. The presented radar achieves the longest vital-sign detection distance among state of the art, while consuming at least 100× less power, enabling many battery-powered and handheld radar sensing applications.

References:

[1] N. Andersen et al., "A 118mW Pulse-Based Radar SoC in 55nm CMOS for Non-Contact Human Vital Signs Detection," *IEEE JSSC,* pp. 3421-3433, Dec. 2017.
[2] T.-S. Chu et al., "A Short-Range UWB Impulse-Radio CMOS Sensor for Human Feature Detection," *ISSCC,* pp. 294-296, 2011.
[3] L. Lou et al., "A 253mW/Channel 4TX/4RX Pulsed Chirping Phased-Array Radar TRX in 65nm CMOS for X-Band Synthetic Aperture Radar Imaging," *ISSCC,* pp. 160-162, 2018.
[4] Y. Wong et al., "A 260mW Ku-Band FMCW Transceiver for Synthetic Aperture Radar Sensor with 1.48GHz Bandwidth in 65nm CMOS Technology," *IEEE T-MTT,* pp. 4385-4399, Nov. 2017.
[5] H. Yeo et al., "A 940MHz-Bandwidth 28.8ms-Period 8.9GHz Chirp Frequency Synthesizer PLL in 65nm CMOS for X-band FMCW Radar Applications," *ISSCC,* pp. 238-240, 2016.

 978-1-5386-8531-0/19/$31.00

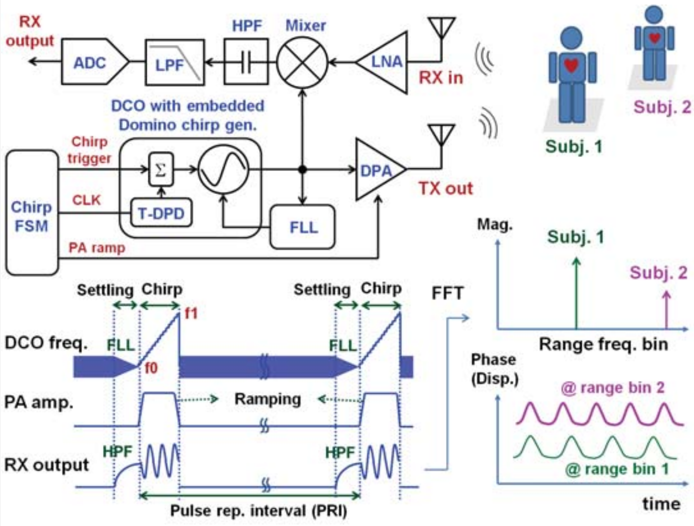

Figure 9.3.1: Simplified block diagram and concept illustration of the proposed burst-chirp radar.

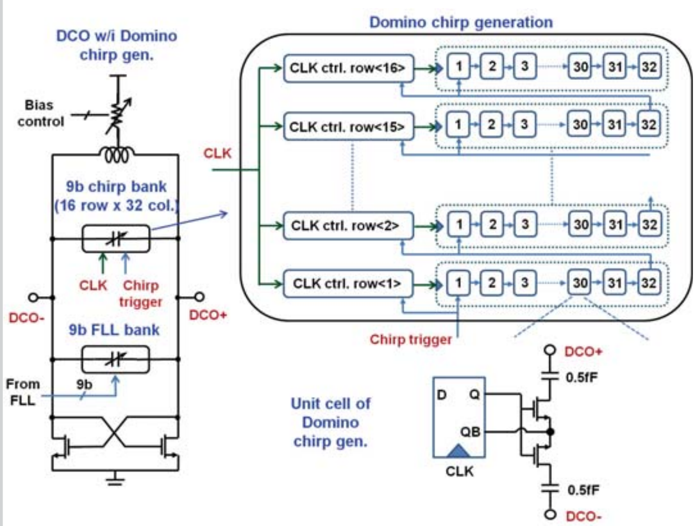

Figure 9.3.2: Simplified schematic of the DCO with Domino chirp generation.

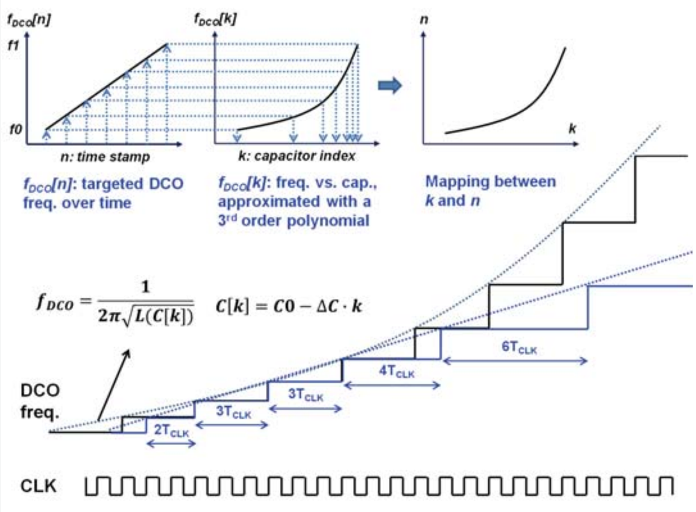

Figure 9.3.3: Concept illustration of the proposed time-domain chirp pre-distortion (with exaggeration).

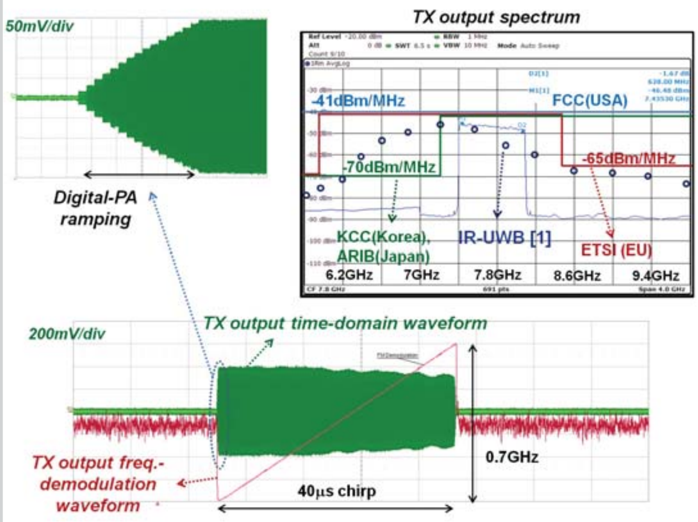

Figure 9.3.4: Measured time-domain waveforms of TX burst and frequency demodulation, and the TX output spectrum.

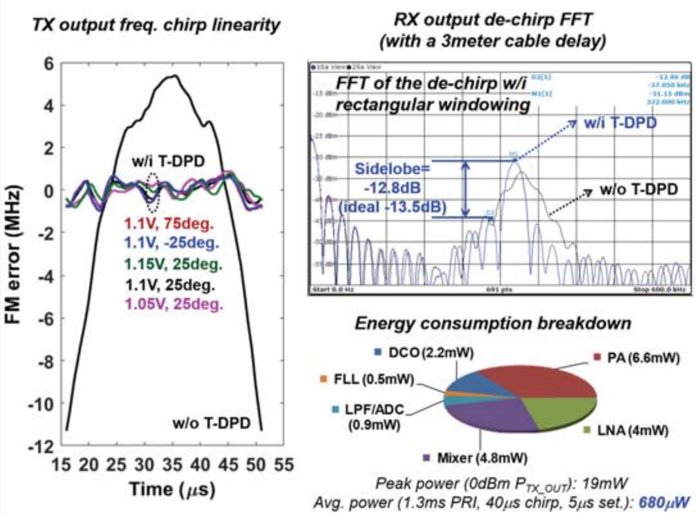

Figure 9.3.5: Measured chirp frequency non-linearity, RX output de-chirp FFT, and the peak power consumption breakdown.

	This work	[1] Andersen, JSSC'17	[2] Chu, ISSCC'11	[3] Lou, ISSCC'18	[4] Wang, JSSC'17	[5] Yeo, ISSCC'16
Tech.	40nm	55nm	130nm	65nm	65nm	65nm
Freq. (GHz)	6.8-8.2GHz	7.2-8.5GHz	2-5GHz	10GHz	15GHz	8.4-9.4GHz
UWB indoor regulation Compliancy	FCC/ETSI/ KCC/ARIB	FCC/ETSI/ KCC/ARIB	N.A.	Outdoor	Outdoor	-
UWB sideband PSD	**-85dBm/MHz**	-70dBm/MHz	-	-	-	-
Modulation	Burst chirp	Impulse	Impulse	FMCW saw-tooth*	FMCW saw-tooth	FMCW triangular
VDD	1/1.1V	1.8V	1.9V	1.2V	1.2V	1.1-1.3V
Mod. BW	0.7-0.8GHz	1.4GHz	0.9GHz	1GHz	1.48GHz	0.95GHz
Pulse/chirp period	10-40μs	1.8ns	3ns	0.2-1ms	1-10ms	28μs
Pulse rep. interval	1.3ms	N.A.	100ns	1ms	1-10ms	28μs
TX P_{OUT}	0dBm	0.7dBm	N.A.	10dBm	13dBm	-
TX RMS freq. error	0.3-0.5MHz	-	-	0.2-1.1MHz	0.16MHz	1.7MHz
RX FFT sidelobe	-12.8dB	-	-	-12.9dB	-12.7dB	-
Heartrate det. distance	5m	5m	-	-	-	-
Breath det. distance	**15m**	9m	0.75m	-	-	-
Die area	**1.8mm²**	8.6mm²	11.9mm²	7.8mm²	4mm²	0.18mm²***
Peak DC power: Chirp gen.	**2.7mW**	11.5mW	N.A.	N.A.	41mW	14.8mW
Peak DC power: Total	**19mW**	N.A.	N.A.	141mW/ch**	148mW**	-
DC power active det.	**<0.68mW**	118mW	695mW	141mW/ch**	148mW**	14.8mW***

* Non-continuous saw-tooth chirp for synthetic aperture radar, but the radar is continuous active.
** PA power consumption is excluded for fair comparison. *** PLL only.

Figure 9.3.6: Summary and comparison table of state-of-the-art IR-UWB and X-band FMCW radars.

9

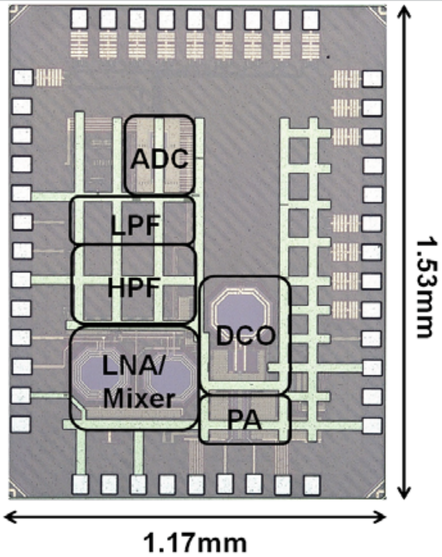

Figure 9.3.7: Die micrograph.

 978-1-5386-8531-0/19/$31.00